



World Journal of Engineering

An improved integrated control modeling of a high-power density interleaved non-inverting buck-boost DC-DC converter

Mohsen Karimi, Mohammad Pichan, Adib Abrishamifar, Mehdi Fazeli,

Article information:

To cite this document:

Mohsen Karimi, Mohammad Pichan, Adib Abrishamifar, Mehdi Fazeli, "An improved integrated control modeling of a high-power density interleaved non-inverting buck-boost DC-DC converter", World Journal of Engineering, <https://doi.org/10.1108/WJE-11-2017-0360>

Permanent link to this document:

<https://doi.org/10.1108/WJE-11-2017-0360>

Downloaded on: 04 November 2018, At: 20:53 (PT)

References: this document contains references to 0 other documents.

To copy this document: permissions@emeraldinsight.com

The fulltext of this document has been downloaded 1 times since 2018*

Access to this document was granted through an Emerald subscription provided by emerald-srm:380143 []

For Authors

If you would like to write for this, or any other Emerald publication, then please use our Emerald for Authors service information about how to choose which publication to write for and submission guidelines are available for all. Please visit www.emeraldinsight.com/authors for more information.

About Emerald www.emeraldinsight.com

Emerald is a global publisher linking research and practice to the benefit of society. The company manages a portfolio of more than 290 journals and over 2,350 books and book series volumes, as well as providing an extensive range of online products and additional customer resources and services.

Emerald is both COUNTER 4 and TRANSFER compliant. The organization is a partner of the Committee on Publication Ethics (COPE) and also works with Portico and the LOCKSS initiative for digital archive preservation.

*Related content and download information correct at time of download.

An improved integrated control modeling of a high-power density interleaved non-inverting buck-boost DC-DC converter

Abstract

Purpose – This paper proposes a novel integrated control method (ICM) for high power density non-inverting interleaved buck-boost DC-DC converter. In order to achieve high power conversion by conventional single phase DC-DC converter, inductor value must be increased. This converter is not suitable for industrial and high power applications since large inductor value will increase the inductor current ripple. Thus, two-phase non-inverting interleaved buck-boost DC-DC converter is proposed.

Design/methodology/approach –The proposed ICM approach is based on the theory of integrated dynamic modeling of continuous conduction mode (CCM), discontinuous conduction mode (DCM) and synchronizing parallel operation mode. In addition, it involves the output voltage controller with inner current loop (inductor current controller) to make a fair balancing between two stages. To ensure fast transient performance proposed digital ICM is implemented based on a TMS320F28335 digital signal microprocessor (DSP). The experimental results from test bench of 30kW non-inverting interleaved buck-boost DC-DC converter with large input voltage variation (70-160VDC) and output voltage regulation (110VDC) is provided to evaluate the performance of the proposed ICM.

Findings – The results verify the effectiveness of the proposed ICM algorithm to achieve high voltage regulating (under 0.01%), very low inductor current ripple (for boost is 1.96%, for buck is 1.1) and fair input current balance between two stages (unbalancing current less than 0.5A).

Originality/value – The proposed new ICM design procedure is developed satisfactorily to ensure fast transient response even under high load variation and the solving RHP zeros of the CCM. In addition, the proposed method can equally divide the input current of stages and stable different parallel operation modes with large input voltage variations.

Keywords- DSP controller, Integrated control system (ICM), Non-Inverting Interleaved buck-boost DC-DC converter, Operating-mode optimization of converter, Steady state analysis of the INBB converter

Paper type – Research paper

1. Nomenclature

L	-Inductor
V_{in}	-Input Voltage
V_{out}	-Output Voltage
I_{out}	-Output Current
C	-Output Capacitor
R	-Output Resistance
D_{boost}	-Duty Cycle of Boost Switch
D_{buck}	-Duty Cycle of Buck Switch
$D_{buck-boost}$	-Duty Cycle of Buck and Boost Mode
ΔI_{L1}	-Current Ripple of First Stage
ΔI_{L2}	-Current Ripple of Second Stage
I_{L1}	-Inductor current of First Stage
I_{L2}	-Inductor current of Second Stage
F	-Switching Frequency
$V_o(0)$	-Large Signal of Output Voltage

$\tilde{V}_o(0)$	-Average of output voltage
N	-The Number of Parallel Stage
G_{PL}	-The Trance Function of PI Controller
K_P	-Gain of Proportional
K_I	-Gain of Integral
K_d	-Gain Value of Output Voltage
G_C	-Transfer Function of controller
G_P	-Transfer Function of controller
$T_V(s)$	-Circuit of Digital Power Manger

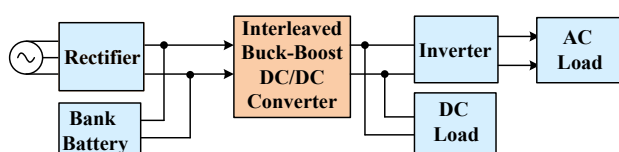
2. Introduction

The buck-boost DC-DC converters are mandatory to supply for critical load that provided a regulated output DC voltage from a variable voltage and different sources. Hence, they are used widely in industrial applications such as uninterruptible power supplies (UPSs), wind energy conversion, solar power plants, etc. The non-inverting buck-boost DC-DC converter generates a regulated energy to the load from above (buck mode) or below (boost mode) or

equal (buck-boost mode) than the source voltage by modify operation modes of the converter. Also, it can be used to combine different types of energy resources (Young *et al.*, 2009; Robert *et al.*, 2014; Mahdi *et al.*, 2015; Seyed *et al.*, 2017). Recently, several topologies have been proposed for this purpose. The flyback and buck-boost inverting converters are suitable for low voltage and low output current or low power applications (H *et al.*, 2004). However, in high voltage applications, a lot of stress is applied to the switches in the changing operation modes. The Cuk and SEPIC converters have additional two pairs of inductor and capacitor (Guoliang and Wentao, 2007). Therefore, according to usage of more devices, the converter will be inefficient and costly (H *et al.*, 2012). The other disadvantage of Cuk and buck-boost inverting converters is that the output does not serve the needs of applications where a positive output voltage is required (Amin *et al.*, 2015). It is worth mentioning that the size of the inductor is also important to the DC-DC converter (Andersen and Blaabjerg, 2006; Ahmad *et al.*, 2017). In order to achieve high power density of the DC-DC converter, the two-phase interleaved non-inverting buck-boost DC-DC converter (INBB) is proposed. This topology offers several advantages such as achieving high power conversion without resizing the inductor well as same capacitor, similar to the single phase system. The INBB DC-DC converter is a cascaded connection of the buck and boost converters that combine two stages of buck-boost converter in parallel and just one capacitor bank is shared between both stages. In addition, this converter reduces weight and cost compared to other converters as well as the topology is very compatible for industrial applications (Garate *et al.*, 2015). Figure 1 shows the schematic of uninterruptible power supply (UPS) including the INBB DC-DC converter. The INBB DC-DC converter is used between the rectifier and inverter for protecting the high critical loads to provide high reliable DC power source for inverter. The proposed INBB DC-DC converter is equally divided the input current among the stages. The advantage of the proposed converter is summarized as follow:

- Achieving high power DC-DC converter without changing the inductor size,
- High regulating accuracy of the output voltage with large input source variation,
- Low inductor current ripple results in reduced switching losses of the converter and provides higher efficiency.

Figure 1 The schematic of common UPS with high reliable DC power source



The rest of this paper is organized as follows: Section II discusses the structure of INBB DC-DC converter and

presents different operation modes and analyzed the steady state operation of the converter. Analyzing the proposed ICM for the two-phase INBB converter is described in section III. Simulation and experimental results of the INBB converter with ICM are provided, respectively, in section IV. Finally, the conclusions of this study are presented in Section V.

3. Structure of two-phase INBB DC-DC converter

One of the most significant characteristic of this converter is the fast transient response in changing between different modes. In particular is worth mentioning that, when the converter operates in CCM boost mode, a right-half-plane (RHP) zero is appeared. Thus, the controller design is complicated greatly due to different operation modes and the bandwidth limitation of the control. Various control methods were proposed to solve the mentioned problems and regulating the output voltage of the DC-DC converter (Apparao and Venkata, 2017; Amin *et al.*, 2015). However, the conventional controllers implementation are not feasible with different modes and even parallel operations with input current balancing among stages (Alireza *et al.*, 2015). The proposed ICM design is developed satisfactorily to have fast transient response under high load variation as well as solving RHP zeros of the CCM. In addition, the proposed method can equally divide the input current of stages and stable different parallel operation modes with large input voltage variations. The proposed ICM involved three loop compensators including one voltage loop and two current loops. The proposed ICM is absolutely integrated the individual operation of the compensators. Also, it is accurately generated the duty cycles for the paralleled switches which are phase shifted by 180 degree from each other.

Accordingly, the result of ICM is significantly reduced the inductor current ripples flowed to output, that considerably reduces the output voltage ripple. Therefore, the ripple value is decreased by half of the total current ripple flowing into the output capacitor. Consequently, the voltage stress of switches decreased which considerably reduces values of the passive elements and switching time delay. Furthermore, the new ICM offers the best and simplest integration of multiple operation modes. To sum up, the proposed ICM exhibits superior performance under different operation modes, greatly improves the transient response and finally considerable small EMI filter.

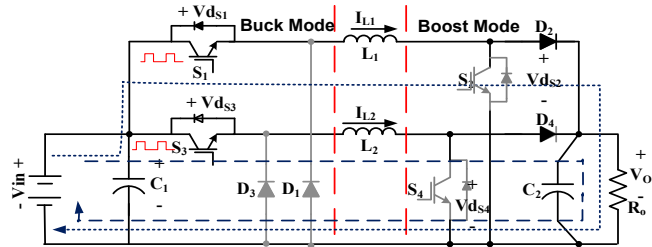
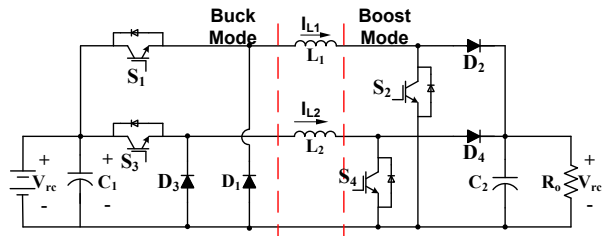
3.1 Operating-mode optimization of two-phase INBB converter

The proposed topology is shown in Figure 2. This INBB DC-DC converter can be paralleled different modes such as boost, buck or buck-boost modes. The INBB converter consists of switches S_1 & D_1 for 1st stage and S_3 & D_3 for second stage in parallel buck operation modes. The boost mode operates only with switches S_2 & D_2 of 1st stage and S_4 & D_4 of 2nd stage or buck-boost converter. The inductor L_1 is connected between D_1 & S_2 , and L_2 is connected between D_3 and S_4 while D_2 and D_4 are connected to output capacitor.

The L_1 & L_2 are shared with both buck and boost modes operations.

Figure 2 The interleaved technique for non inverting buck-boost converter configuration

Figure 3 Equivalent circuits of converter when S_1 & S_3 = PWM and S_2 & S_4 = OFF in the buck mode



Continuous conduction mode (CCM) operation: A 180° phase shift is done between the switching signals of the first stage and the second stage. The operation of the INBB DC-DC converter when $V_{in} > V_{out}$ under high loads are shown in Figure 3 and 4, respectively. The key waveform of CCM operation in once period of switching is shown in Figure 7. At time period t_0 , the switches S_1, S_3 shown in Figure 3 are turned ON and D_1, D_3, S_2, S_4 are turned OFF; while inductor currents; I_{L1} and I_{L2} increased linearly from DC source voltage. At t_1 the inductor (L_2) energy is stored to the capacitor C_2 , and L_1 continues to increase energy storage, and at instance t_3 the inductor energy L_1 is stored to the capacitor C_2 . Therefore, the variations of I_{L1} and I_{L2} are concluded as follow;

$$I_{L1} = \frac{V_{L1}}{L1} (t_3 - t_0) = \frac{V_{in}}{L1} \cdot DT_S \quad (1)$$

$$I_{L2} = \frac{V_{L2}}{L2} \cdot (t_3 - t_0) = \left(\frac{V_{in}}{L2} - \frac{V_{out}}{L2} \right) \cdot DT_S \quad (2)$$

At second time period t_4 , S_1, S_3, S_4, D_1, D_2 are turned OFF and S_2, D_3, D_4 are turned ON. L_1 energy is discharged to output capacitor and L_2 energy is increased by input source. Thus, the I_{L1} and I_{L2} currents are obtained as follow:

$$I_{L1} = \frac{V_{L1}}{L1} (t_4 - t_3) = -\frac{V_{out}}{L1} \cdot DT_S \quad (3)$$

$$I_{L2} = \frac{V_{L2}}{L2} (t_4 - t_3) = \left(\frac{1}{3} \cdot \frac{V_{in}}{L2} \right) \cdot DT_S \quad (4)$$

Due to the symmetry of the circuit, periodically this circuit repeats at all the time of operation modes. Totally, the ripple of I_{out} is equal to sum of I_{L1}, I_{L2} regarding two parallel operations.

Figure 4 Equivalent circuits of converter when S_1 & S_3 = OFF and S_2 & S_4 = OFF in the buck mode when L is discharged

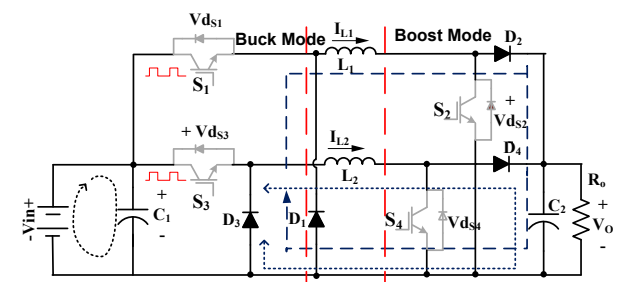


Figure 5 Equivalent circuits of converter when S_1 & S_3 = ON & S_2 & S_4 = PWM and D_1 & D_3 = OFF in boost mode when L is charged (load supplied by C_2)

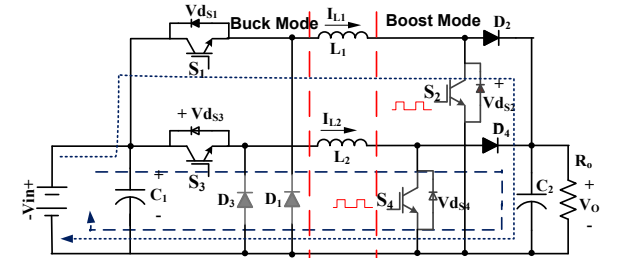


Figure 6 Equivalent circuits of converter when S_1 & S_3 = ON and S_2 & S_4 = PWM in boost mode when L is discharged

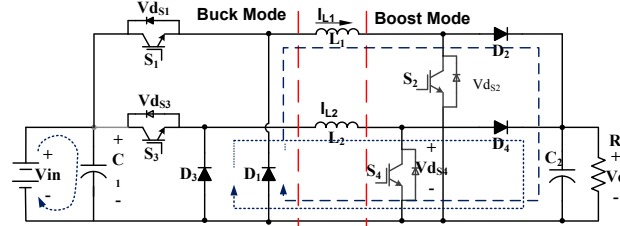
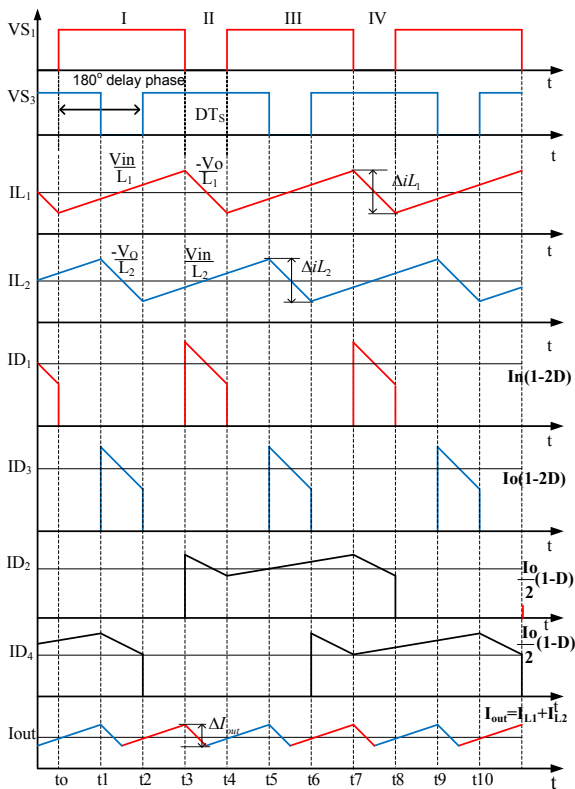


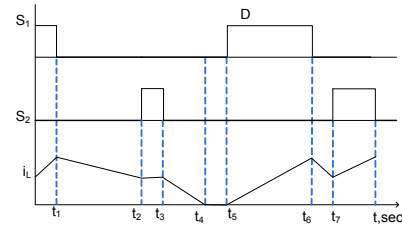
Figure 7 Key waveforms operations



Discontinuous conduction mode (DCM) operation:

According to output power, the converter must be supplied wide range of output load, when the density of load is low in the high switching frequency, the converter operates in the DCM. When the load is high, the converter operates in the CCM. At t_2 when $V_{in} < V_{out}$, S_1 & S_3 have always been ON and S_2 & S_4 are turned PWM (shown in Figure 6 and Figure 7). In these operation modes, inductors L_1, L_2 stored energy from source V_{in} . The load is supplied by output capacitor (C_o). The problem of DCM operation is corresponded with decreasing I_{L1} & I_{L2} to zero caused high stress-switches during current turn-off condition. Regarding the proposed interleaved topology in this paper, when I_{L1} & I_{L2} adds together to the output current I_{out} , the zero crossover of average ΔI_L is eliminated. Thus, the switching frequency can be chosen less than conventional method. And according to parameters of converter and requirement of efficiency the switching frequency is chosen 12 kHz. In other, the very high frequency is increased the stress of switches and switching loss. Therefore, the control of essential parameters of converter such as critical parameter, operation in different modes, fast dynamic response and efficiency is become more complex. The inductor current waveform of single non-inverting buck boost converter is shown as Figure 8. At the time period t_2 , inductor current increases I_L linearly, and at t_3 , I_L decreases to zero during same switching cycle, when it changes from CCM to DCM. Thus, in this mode, the total ripple inductors current ΔI_{out} decreases linearly.

Figure 8 Waveforms under DCM operation at t_2



The main goal of proposed the ICM is applied to the two-phase INBB converter for achieving fast transient response of different dynamic modeling without changing the algorithm of controller and any additional component. The phase-delay between modules is shown in Figure 9a. This system uses two PWM modules, with triangle carrier T_1 configured as the master and T_2 configured as a slave. The delay phase F between T_1 and T_2 must be $F = 180^\circ$. The slave module is synchronized to the master first module. In any operation mode of converter always one switch is ON and the second parallel switch is off at the same time which forms the complementary operation of two stages. Hence, the equivalent circuit diagram of the first stage which its switch is "ON" is different with the second parallel stage (its parallel switch is OFF) of the converter. Therefore, at the same period time, first stage stores energy in relative inductor and the second parallel stage transfers the stored energy of its inductor to the output capacitor and this procedure is repeated again. Thus, the equations of the equivalent circuit diagram of first stage are repeated for the second parallel stage.

The result of comparing duty cycle of each operation mode is shown Figure 9a and the simulation implementation of PWM for buck and boost modes in parallel operation are shown in Figure 9b.

$$\begin{aligned} \text{If } V_{in} < V_{ref} : D_{controller} < 1 &\longrightarrow D_{controller} = D_{BOOST} \\ \text{If } V_{in} > V_{ref} : D_{controller} < 1 &\longrightarrow D_{controller} = D_{BUCK} \\ \text{If } V_{in} = V_{ref} : D_{controller} < 1 &\longrightarrow D_{controller} = D_{BUCK-BOOST} \end{aligned}$$

Figure 9a PWM pulse generation

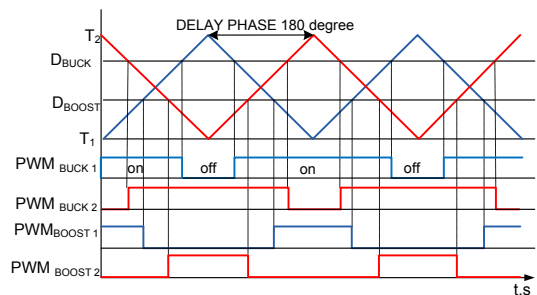
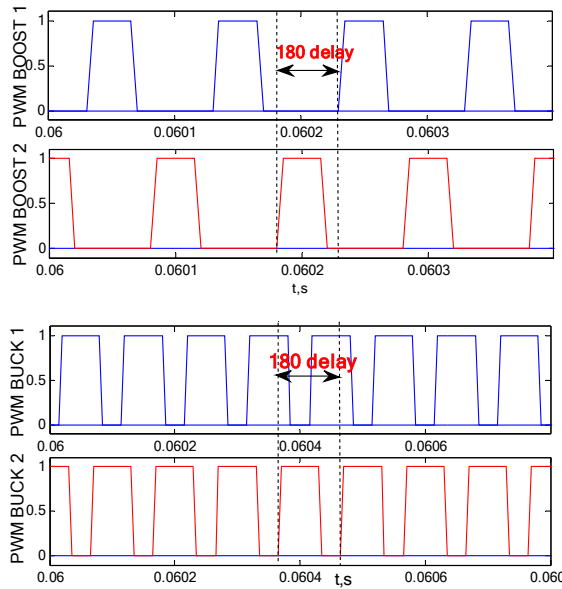


Figure 9b PWM pulse generation for two stage parallel in boost and buck operation modes



3.2 Steady State Analysis of the INBB converter

The design of the two-phase INBB converter is the same like the conventional single non-inverting buck-boost converter. This converter can operate as a buck by switch S_1 & D_1 and also operate as a boost converter by switch S_2 & D_2 and in the middle voltage the converter operates as buck-boost mode by switches S_1 & S_2 . The steady state transfer function is used large and small signal and analysis based on state space averaging method [15-18]. All operation modes of the INBB converter in steady state are used principle of inductor volt-second balance and capacitor charge balance. The duty cycle D and output voltage are obtained as given in the following expression.

A. Buck mode ($V_{in} > V_{out}$): The duty cycle of converter in buck operation modes is obtained as follows.

where V_{in} is the input source voltage and V_{out} is the output voltage of converter.

$$D_{buck} = \frac{V_{out}}{V_{in}} \quad (5)$$

$$\frac{dV_{out}}{dt} = \frac{1}{C} \left(i_L - \frac{V_{out}}{R} \right) \quad (6)$$

$$\frac{di_L}{dt} = \frac{1}{L} (V_{in} - V_{out}) \quad (7)$$

The transfer-function of buck operation is combined equation. 5, 6, 7 yields (8):

$$\frac{\%o(s)}{D_{buck}(s)} = \frac{\frac{1}{L \cdot C} \cdot V_{in}}{s^2 + \frac{s}{R \cdot C} + \frac{1}{L \cdot C}} \quad (8)$$

The value inductor current for buck mode is obtained as follows.

$$L_1 = L_2 = \frac{(V_{in_{max}} - V_{out}) \cdot V_{out}}{V_{in_{max}} \cdot r \cdot f \cdot I_{out}} \quad (9)$$

where "r" is current difference ratio between inductor current ripple and output current.

$$r = \frac{\Delta I_L}{I_{out}} \quad (10)$$

therefore, "r" is set in the range of 0.25–0.5 and where ΔI_L is ripple inductor.

B. Boost mode ($V_{in} < V_{out}$): The operation is divided into two modes of operation corresponding to switches S_2 & S_4 , according to phase shift delay in the beginning of PWM. When the switch S_2 is closed and S_1 is ON as shown in Figure 5 and Figure 6. The diode D_2 is reverse biased and the input energy stored in the inductor L_1 while the load supplies by the capacitor C_2 . The dynamic equations of the converter are obtained as

$$L \frac{di_L}{dt} = V_{in}(t) \quad (11)$$

$$\frac{dv_c}{dt} = \frac{1}{C} \cdot \left(-\frac{V_c}{R} \right) \quad (12)$$

In the second operation modes, the switch S_2 is OFF, and S_1 is ON as shown the Figure 6. The diode D_2 conducts and both energy from the input voltage and energy stored in the inductor, then are discharged to the capacitor and the load. The dynamic equations of the converter are shown as follows (3)

$$L \frac{di_L}{dt} = V_{in}(t) - (1 - D_{boost}(t)) \times V_{out}(t) \quad (13)$$

Regarding Laplace method, from the Figure 5 the output voltage corresponding to boost mode operation is adjustable via the duty cycle D_{BOOST} as given in the following expression.

$$\frac{\%o(s)}{D_{boost}(s)} = \frac{\%o \cdot (1 - D_{boost}) - \frac{sI_L}{C}}{s^2 + \frac{s}{RC} + \frac{(1 - D_{boost})^2}{LC}} \quad (14)$$

The value of inductor L_1 and L_2 is equal. Thus the minimum inductors value are given by

$$L_1 = L_2 = \left(\frac{(V_{out} - V_{in_{min}}) \cdot V_{out}}{V_{in_{min}} \cdot f \cdot V_{out}} \right) \quad (15)$$

Duo to the proposed interleaved converter, the ripple currents of inductor ΔI_{L1} and ΔI_{L2} are symmetrical.

$$\Delta I_{L_1} = \Delta I_{L_2} = 0.4 \cdot \frac{I_{out}}{2} \cdot \frac{V_{out}}{V_{in_{max}}} \quad (16)$$

The output capacitor is sharer for the two-phase INBB converter, which is calculated using expression below.

Where ΔV is 0.1% of the value output voltage. And where, f is total switching frequency.

$$C_{out} = \frac{I_{out} \cdot D_{max}}{f \cdot \Delta V} \quad (17)$$

C. Buck-boost mode ($V_{in} = V_{out}$): For buck-boost operation modes, the transfer-functions and DC-gains are (18),(19),(20),(21).

$$\frac{\%o(s)}{D_{buck-boost}(s)} = \frac{\left(\frac{V_{in} + \%o}{L \cdot C}\right) \cdot (1 - D_{buck-boost}) - \frac{sI_L}{C}}{s^2 + \frac{s}{RC} + \frac{(1 - D_{buck-boost})^2}{LC}} \quad (18)$$

And therefore

$$V_O(0) = \frac{\left(\frac{V_{in}}{L \cdot C}\right) \cdot (1 - D_{buck-boost})}{s^2 + \frac{s}{RC} + \frac{(1 - D_{buck-boost})^2}{LC}} \quad (19)$$

Hence

$$\frac{\%o(s)}{D_{buck-boost}(s)} = \frac{(V_{in} + V_{out})}{(1 - D_{buck-boost})} \quad (20)$$

The output voltage of converter in buck-boost modes is obtained the following

$$V_O(0) = \frac{D_{buck-boost} \cdot V_{in}}{(1 - D_{buck-boost})} \quad (21)$$

When the INBB converter is operated in the steady state, the duty cycle of the proposed converter can be obtained as follows

$$\frac{V_o}{V_{in}} = \frac{2 \cdot D_{buck-boost}}{(1 - D_{buck-boost})} \text{ then } \frac{V_o}{V_{in}} = \frac{N \cdot D_{buck-boost}}{(1 - D_{buck-boost})} \quad (22)$$

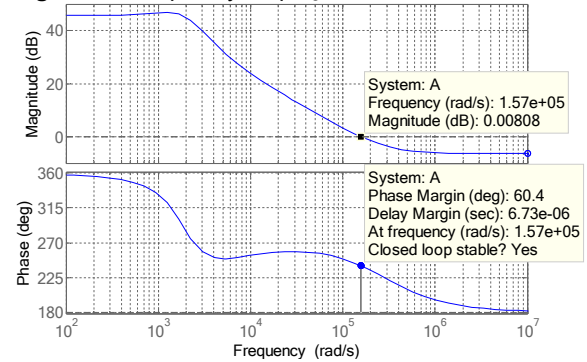
4. Integrated control modeling (ICM) technique for INBB converter

4.1 Analyzing the proposed ICM of the two-phase INBB converter

The Bode diagram of single converter shows that the phase margin is not enough for stability of converter. It is nature of non-inverting buck boost converter. Hence, the controller must be increased the phase margin. The problems of designing the controller is that zero of the system limits the bandwidth of loop-control. The Bode plot of non-inverting

buck boost converter is illustrated on Figure 10. The phase margin of close loop system is about 60 degree, therefore for stability of the closed loop cut-off frequency should be much smaller than pole frequency, so that means the crossover frequency has to choose high for necessary available loop bandwidth. Hence, the phase margin can be covered the close-loop system's stability.

Figure 10 Frequency responses of V_{out}/V_{in}



The phase margin of the loop gain should be positive implies that the system is stable. The value of phase margin is 45° to 60° corresponding to stability is suitable. A proportional-integral (PI) controller is used to increase the low frequency loop gain, thus reducing steady-state error to guarantee stability. The transfer function of a PI controller is shown in (23).

$$G_{PI}(s) = Kp + \frac{KI}{s} \quad (23)$$

In the last previous literature, for CCM and DCM operation is required individual two controllers (Young. *et al.*, 2009; Robert *et al.*, 2014; Mahdi *et al.*, 2015; Seyed *et al.*, 2017; Z *et al.*, 2005; H *et al.*, 2016; Liqin *et al.*, 2012). Therefore, the problem is choosing the appropriate controller for different operation modes. During transient modes, the controller must be changed. Therefore, changing the controller may change the dynamic response of converter to deterioration. A novel ICM is proposed for control system of the two-phase INBB converter. The proposed controller is integrated at all the different operating modes such as buck, boost, and buck-boost, CCM and DCM. The ICM are also controlled the main function of the converter such as adjusting delay phase of switching, limitation of current inductors ripple, regulation output voltage due to large variation of source, fast transient response. Figure 11 shows the circuit of control system. The proposed ICM of two-phase INBB converter is consisted of three loop controllers, which are the voltage loop controller for regulating output voltage and the two independent inner current loop controllers which are designed especially for eliminating of inductors current ripple according to each stage has own current sensor. Moreover, the current controllers are getting the same desired values I_{L1} & I_{L2} . In the Figure 11, the current reference I_{ref} is produced by voltage controller that the both master and slave current controllers are fed by I_{ref} . The

switches S_3, S_4 of slave phase are always controlled by interleaving circuit with time delay 180° . The master phase never used the inductor current I_{L2} of slave phase. Therefore, each current controller has a current limit circuit for more protection. Each phase has the own current controller, which are generated the duty cycle of switches depending on the mode transition. The novelty of the ICM is to distinguish the mode transition without any changing in dynamic response and additional any component. However, when the converter begins to operate, the ICM is determined the duty cycle of controller $D_{control}$ to achieve the required output and can be taking the value among $0 \sim 2$. If $V_{in} > V_{out}$ the ICM is put the value $D_{control} = 0 \sim 1$. According to equations (24-25), the duty cycle of the buck switches is equal to $D_{control}$ and the duty cycle of the boost switches equal zero because in the buck modes the value $D_{control}$ is less than "1". Therefore, the amount duty cycle of the boost switches from equation (25) becomes negative. Consequently, the negative duty cycle is not defined and is equal to zero " $D_{boost} = 0$ ", and the boost switches is kept off. In the boost operation modes the ICM is kept maximum rate of duty cycle $D_{control} > 1$, the duty cycle of buck switches always is kept "1". The duty cycle of boost mode can be determined as equation (25) $D_{boost} = 1 - D_{control}$. Consequently, the integrated controller is determined the duty cycle D which can be found as following:

$$D_{BUCK} = D_{controller} \quad (25)$$

$$D_{BOOST} = \begin{cases} 0 & \text{if } D_{controller} < D_{BUCK} \\ D_{controller} - 1 & \text{if } D_{controller} > D_{BUCK} \end{cases} \quad (26)$$

$$D_{BUCK-BOOST} = \begin{cases} D_{controller} - 1 & \text{if } D_{controller} > D_{BUCK} \\ D_{controller} & \text{if } D_{controller} < D_{BUCK} \end{cases} \quad (26)$$

Figure 11 The ICM of INBB converters

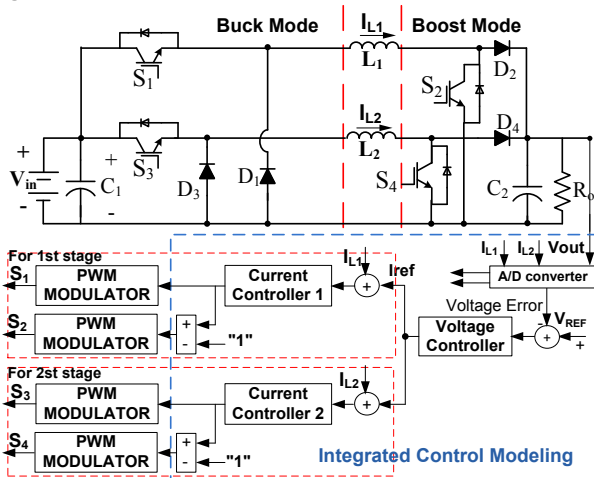
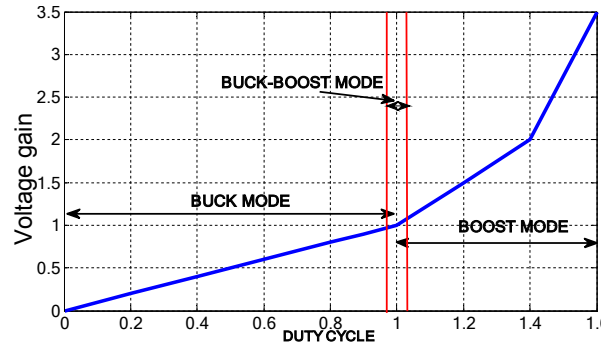


Figure 12 is illustrated the proposed converter is operated continuous among the different modes of operation.

Figure 12 Confine diagram of duty cycles in different operation modes



Due to non-minimum phase characteristic of the INBB converter, the conventional PI controller is not uncertain to stability and satisfactory dynamic response according to load disturbance, large variation source and uncertain parameters. The proposed ICM is used two parallel inner loop controllers which are cascaded with the sharer PI controller. The proposed ICM is covered all disadvantage characteristic of converter, such as the non-minimum phase, elimination inductor current ripple, stability and robustness in large variation of input source and fast dynamic response during changing operation modes.

4.2 Parameter design and implementation of two-phase INBB converter

The digital controller has many advantages to generate multiphase interleaved gate signals. It has good noise immunization, stable performance, flexibility and ability of more complicated control technique which is important in high power application (Z *et al.*, 2005). In addition, regarding the sampling delay of the ADCs, the reaction speed of digital control is much slower than the traditional analog control system (Liqin *et al.*, 2012). The digital controller can be accurately set to reduce or avoid the propagation delay of the saturation in the transition modes and generated PWM simultaneously for balancing the source currents in each phase in high power application. However, the digital controller design of two-phase INBB converter is implemented with the TI's DSP (digital signal processor) TMS320F28335. The algorithm of digital controller is implemented on a DSP for generating gate digital pulses by comparing a triangular carrier wave of 12kHz as shown in Figure 9a.

Widely, if the sampling frequency of a digital controller is selected to be much higher than the control-loop bandwidth, the algorithm approach of digital controller is in Figure 13 since according to sampling frequency is much faster than the switching frequency that is $f_{sw} = 12\text{kHz}$. Thus, the digital controller is adopted and implemented in the proposed research. In Figure 13 the K_d is gain value of output voltage which is obtained from analog scaled output voltage V_{out} , so that

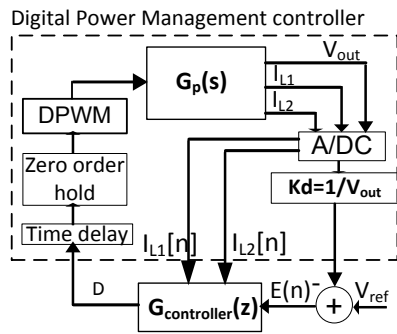
$$Kd = \frac{1}{V_{out}} \quad (27)$$

In the approach DSP based controller, the voltage reference V_{ref} is equal to the nominal output voltage, which is determined by DSP. Then the circuit of digital power management controller is given by

$$T_v(s) = Kd \cdot G_c(s) \cdot G_p(s) \quad (28)$$

where $G_c(s)$ is controller of the converter and $G_p(s)$ transfer function of converter. Due to very high sampling frequency 24kHz is greater than control loop bandwidth below 100 Hz, the digital controller $G_c(z)$ in z domain is selected approximately its $G_c(s)$ controller in s domain.

Figure 13 Digital Control Loop Diagram of two-phase INBB Converter



The electrical specifications are the same as the parameters presented in Table 1 and Figure 1. The second step is to build the state block diagram of the converter by deriving the system model. Figure 14 presents the equivalent circuits of the operating modes in each switching period. The buck operation and boost operation modes are not appeared at the same control period. The two-phase INBB converter of Figure 10 is simulated with the parameters listed in Table I.

TABLE I Prototype parameters

Parameter	Value
V_{in} (VDC)	70~160
V_{out} (VDC)	110
P_{out} (W)	30000
C_s (μ F)	4*2200- 250vdc
$L_{1\&2}$ (μ H)	47
S_1, \dots, S_4	IGBT, 2MBI300U4U
Efficiency	94% @ 100%
DSP	TM320F28335
switching freq., (kHz)	12
Sampling freq., (kHz)	24

The duty cycles of the proposed INBB converter based on the digital implementation individually are produced by

ICM. According to output voltage, the duty cycle for the buck and boost modes can be generated as follows.

where η is the output efficiency of converter.

$$D_{Boost} = 1 - \left(\frac{V_{in_{min}} \cdot \eta}{V_{out}} \right) = 1 - \left(\frac{70 \times 0.95}{110} \right) = 0.39 \quad (29)$$

$$D_{Buck} = \frac{V_{out}}{V_{in_{max}}} = \frac{110}{160} = 0.68 \quad (30)$$

The current ripple ΔI_L of each inductor is

$$\Delta I_L = 0.4 \cdot I_{out} \cdot \frac{V_{out}}{V_{in_{max}}} = 0.4 \times 272 \times \frac{110}{160} = 72.8 A \quad (31)$$

The current ripple ratio "r" is evaluated at maximum load.

$$r = \frac{\Delta I_L}{I_{out}} = 0.275 \quad (32)$$

The equivalent of inductor currents of proposed converter is

$$I_{L1} = I_{L2} = \frac{I_{out}}{2} \quad (33)$$

Thus, the minimum inductor value while the input voltage is high, can be obtained as follows

$$L_1 = L_2 = \left(\frac{(V_{out} - V_{in_{min}}) \cdot V_{out}}{V_{in_{min}} \cdot f \cdot V_{out}} \right) = \left(\frac{(110-70) \times 110}{70 \times 12000 \times 110} \right) = 47 \mu F \quad (34)$$

where ΔV is the desired output voltage ripple and ESR is equivalent series resistance of the used output capacitor.

$$\Delta V = ESR \cdot \left(\frac{I_{out}}{1-D_{Boost}} + \frac{\Delta I_L}{2} \right) = 0.022 \cdot \left(\frac{272}{1-0.39} + \frac{37.4}{2} \right) = 10.22 VDC \quad (35)$$

The output capacitor is sharer for the two-phase INBB converter, which is calculated using expression below

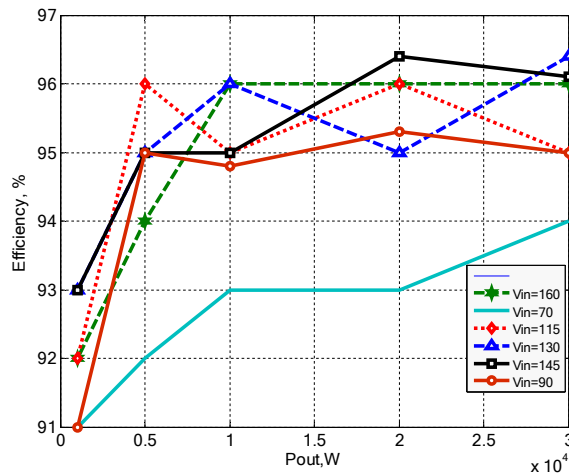
$$C_{out} = \frac{I_{out} \cdot D_{max}}{f \cdot \Delta V} = \frac{272 \times 0.78}{12000 \times 9.8} = 1820 \mu F \quad (36)$$

5. Simulation and experimental results using ICM technique

The total output power of the INBB converter is 30 kW, dividing equally to 15 kW for each stage. The switching frequency of the converter is set to 12 kHz. The output voltage is sampled and converted into digital signal (by A/D converter) and then this sample is compared with the voltage reference to produce the voltage error. The PI controller is analyzed the error signal to produce the current reference I_{ref} for both current controllers and stabilizing the output voltage. The signal I_{ref} is shared to the two current controllers. Figure 14 shows the result of the efficiency comparison through different input voltage

and output power, where the efficiency of the proposed ICM of INBB converter is about 95%. In the buck mode, when the input voltage is in maximum state, the efficiency is reached to 96%. In the boost mode the minimum input voltage also the efficiency is reached 94% at full load 30kW.

Figure 14 Energy conversion efficiency as a function of the output power in the different operation modes: boost mode with $V_{in} = 70, 90$ V, and in buck mode with $V_{in} = 115, 130, 145, 160$ V and $V_{out} = 110$ V



The comparison of efficiencies between different converters was proposed and INBB with ICM are described as table II.

TABLE II Comparison of efficiencies of converter

Topology	$V_{in}(v)$	$V_{out}(v)$	$P_{out}(w)$	$\eta_1(\%)$
Proposed structure	70-160	110	30000	95
(H <i>et al.</i> , 2012)	24-45	28	800	88
(Carlos <i>et al.</i> , 2011)	39-55	48	480	91
(Hafiz <i>et al.</i> , 2016)	70-150	110	300	96
(Liqin <i>et al.</i> , 2012)	163	236	5400	94.9

The efficiency of the proposed converter with ICM is compared with some other existing converter under different output power. The efficiency of existing converters as mentioned was achieved under low power, but the proposed INBB converter has satisfactorily high efficiency under high power density. Figure 16 shows current inductor $I_{L1} + I_{L2}$ and switching signals for boost and buck switches when $V_{in}(t) < V_{out}(t)$. The total inductor presents a reduced current ripple as shown in Figure 15. Figure 16 shows the output voltage and current waveforms with load step change at 0.05s while there is less than 1% ripple in the output voltage because ;

$$\Delta V_{out} = \frac{V_{out_{max}} - V_{out_{min}}}{V_{out}} = \frac{110.04 - 109.92}{110} = 0.001 \quad (37)$$

When $V_{in}(t) > V_{out}(t)$, as shown in Figure 17, the inductor currents $I_{L1} + I_{L2}$ shows low current ripple and switching signals in buck mode (PWM of boost = 0).

Figure 15 Response of output voltage and current in boost mode

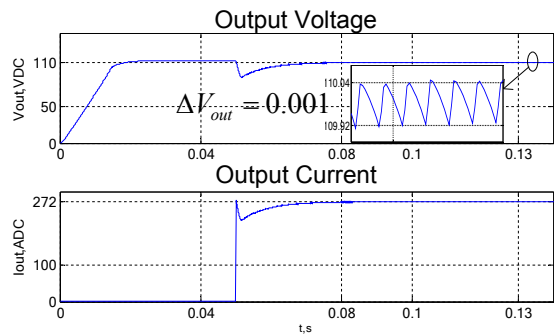


Figure 16 Waveform of Inductor Currents and PWM generation (Dbuck=1, Dboost=0.4, in boost mode)

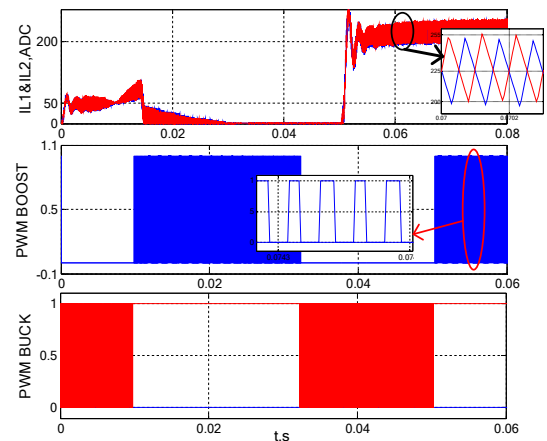


Figure 17 Waveform of output inductors current and PWM in Signal (Dbuck=0.67, Dboost=0, in buck mode)

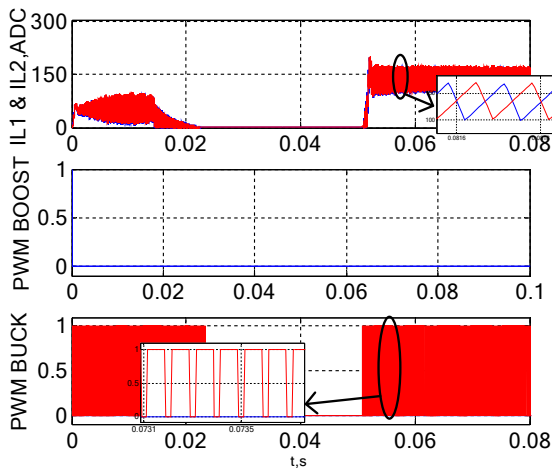


Figure 18a, Figure 18b and Figure 18c show the simulation and experimental results of the output voltage and current waveforms in buck mode transitions with step load from no-load to 100%. The undershoot under the step load charge is very low because the required energy of the output capacitor is supplied through two inductors. The inductors current ripple and input and output voltage of buck mode are shown in Figure 19. The inductors current are followed with 180° delay from each other, which are equal to 72A. Thus, the current balancing is evidently appeared, while the inductors values are identical. The simulation and experimental comparison of the transient from the buck to boost mode is shown in Figure 20a and Figure 20b. Accordingly, the overshoot voltage is equal 6V. Figure 21a and Figure 21b shows the switching signals and inductor currents in buck and boost mode. The PWM of buck switches (S_1, S_3) or boost switches (S_2, S_4) are generated with 180° delay and the inductor currents are synchronized by their PWM. Therefore, the inductor currents are exactly balanced in this operation mode. The output and input voltage and current are shown in Figure 22. The efficiency of the INBB converter in the buck mode can be calculated and is equal 95%. The prototype of INBB converter is illustrated in Figure 23a and Figure 23b that are explained the components of the converter.

Figure 18a Transient response of the output voltage and current in buck mode with step load from 0% to 100%

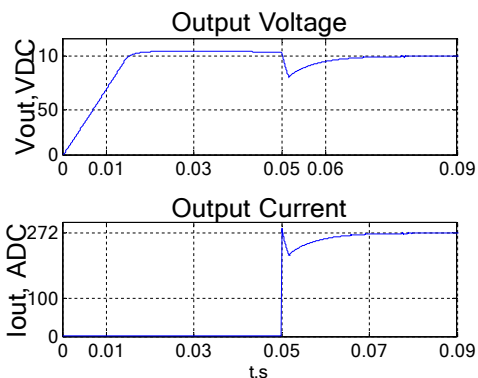


Figure 18b Experimental transient output voltage with step load from 0% to 100% (ch 2: (8.98V/div))

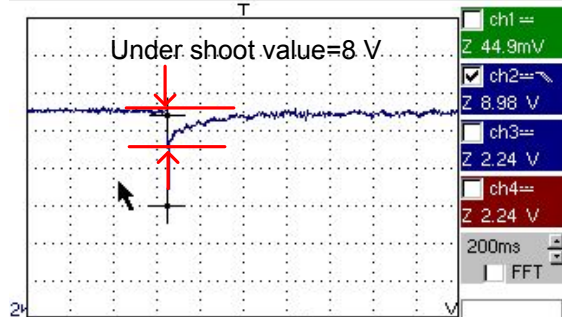


Figure 18c Experimental transient output voltage and current with step load from 100% to 0% of load (ch 1: (50mV/div)), (ch 2: (50V/div))

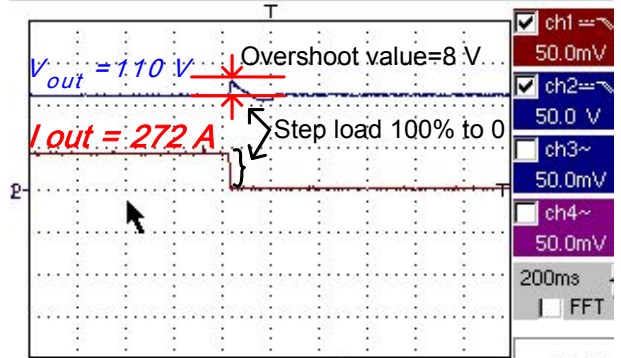


Figure 19 Experimental transient response of inductor currents and input voltage and output voltage under buck mode operation (ch 1-ch 2: (50 V/div)), ch 3-ch 4: (200mV/div))

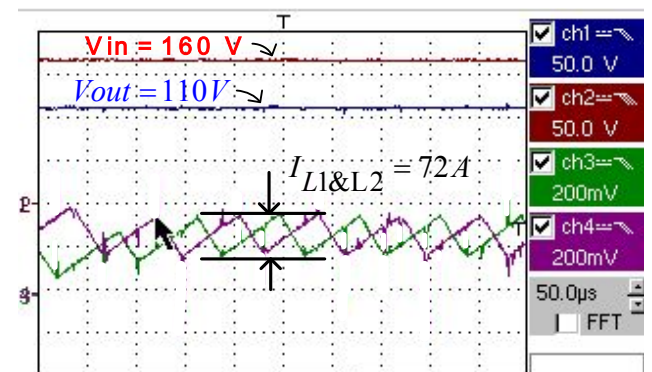


Figure 20a Simulation waveform of transient output voltage from buck to boost

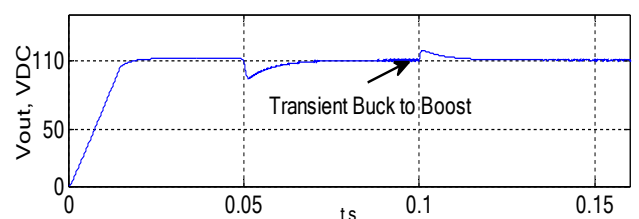


Figure 20b Transient output voltage from boost to buck in full load (ch 1: (50V/div))

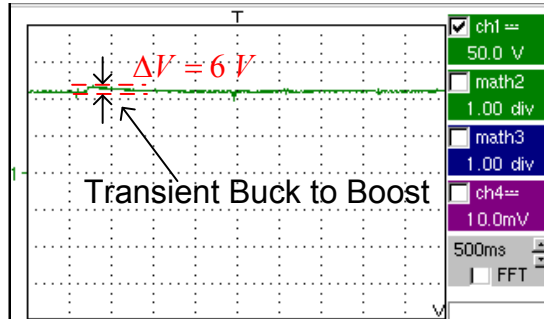


Figure 21a PWM generation and inductor currents under boost mode operation (ch 1-ch 2: (200 mV/div)), ch 3-ch4: (10V/div))

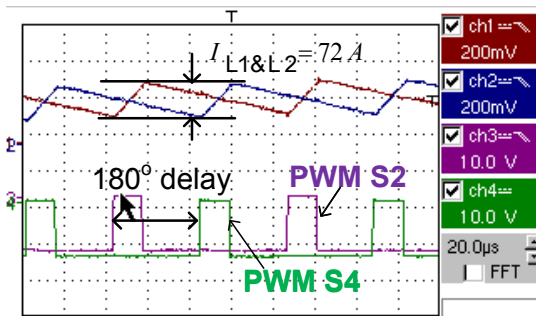


Figure 21b Experimental result of PWM generation and inductor currents under buck mode operation (ch 1-ch 2: (100 mV/div)), ch 3-ch4: (10V/div))

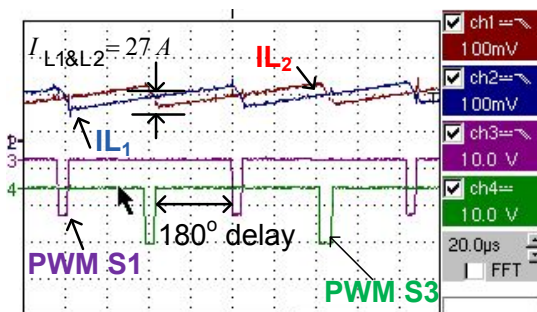


Figure 22 Experimental transient input and output voltages and input current under boost operation mode (ch 1-ch 2: (50 V/div)), ch 3-ch4: (200 mV/div))

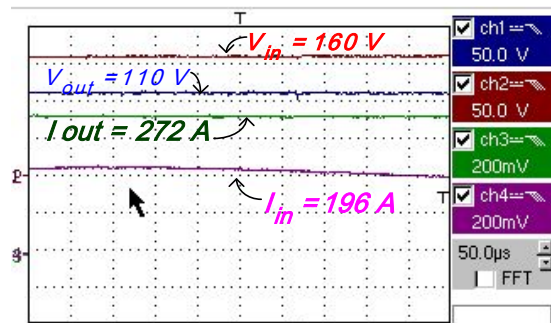


Figure 23a Figure of prototype with DSP (T320F28335)

Figure 23b Figure of prototype INBB DC-DC converter



Figure 23a

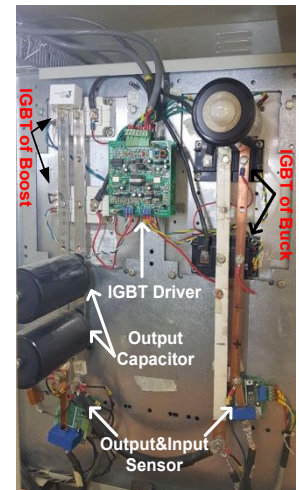


Figure 23b

6. CONCLUSIONS

This paper proposed a new design of ICM for high power density of two-phase interleaved buck boost DC-DC converter. This can be operated flawlessly without changing the dynamic output response in transition modes with the very low inductor ripple, output voltage ripple and low IGBT stresses. The total inductors current ripple has been obtained 50% less than the single converter with the same power. Furthermore, the proposed ICM provides the possibility to be successfully constructed and demonstrated up to the high power density of the converter. Moreover, all simulation and experimental results verify that by employing ICM. A 30kW prototype of interleaved DC-DC converter can be easily converted to a high power density design without increasing components size such as switches, inductor and capacitor. The DSP based ICM was accessed high efficiency 95% under various operating mode transition. Finally, the control strategy is proposed in this paper make the cost lower and improves the conversion efficiency, which makes this method to satisfy considerably higher reliability.

REFERENCES

- Young, L., Alireza, Kh. and Ali, E. (2009), "A Compensation technique for smooth transitions in a non-inverting buck-boost converter", *IEEE Transactions on Power Electronics*, Vol. 24 No. 4, pp. 1002-1016.
- Robert, W.E. and Dragan, M. (2005), "Fundamentals of Power Electronics", *Springer US New York*.
- Mahdi, S., Jafar, S., Adel, Z. and Navid, R.A. (2015), "Hyper-plane sliding mode control of the DC-DC buck/boost converter in continuous and discontinuous conduction modes of operation", *IET Power Electronics*, Vol. 8 No. 8, pp. 1473 – 1482.
- Seyed, M.R., Monazzahalsadat, Y. and Hassan. H.Nia. (2017), "Design of second order sliding mode and sliding mode algorithms: a practical insight to dc-dc buck converter", *IEEE/CAA Journal of Automatica Sinica*, Vol. 4 No. 3, pp. 483 - 497
- H, S.Ch., Wai, L.C and K, S.T. (2004), "A ZCS bidirectional flyback dc/dc converter", *IEEE Transactions on Power Electronics*, Vol. 19 No. 6, pp. 1426-1434.
- Guoliang, C. and Wentao, T. (2007). "Adaptive back stepping control of the uncertain unified chaotic system", *International Journal of Nonlinear Science*, Vol. 4 No. 1, pp. 17-24.
- H, K.L., T, J.L. and J, F.Ch. (2012) "Non-inverting buck-boost converter with interleaved technique for fuel-cell system", *IET Power Electronics*, Vol. 5 No.8, pp. 1379–1388.
- Amin, H., Amir, H.Sh., Navid, N. and David, C.Y. (2015), "Self-tuning indirect adaptive control of non-inverting buck-boost converter", *IET Power Electronics*, Vol. 8, No. 11, pp. 2299 – 2306.
- Andersen, G.K. and Blaabjerg, F. (2005). "Current programmed control of a single-phase two- witch buck – boost power factor correction circuit", *Transactions on Industrial Electronics*, Vol. 53 No. 1, pp. 263 – 271.
- Ahmad, A., Pourya, S., Mehdi, F. and Cihan, H.D (2017), "Chaotic behavior in high-gain interleaved dc-dc converters", *Elsevier, Procedia Computer Science*, Vol. 10, pp. 408–416.
- Garate, J.I., Ibarra, E. and Alegria, I.M. (2015). "Analysis of DC-DC power supply systems for pulsed loads from green electronics perspective", *IET Power Electronic*, Vol. 8 No. 6, pp. 957 – 966.
- Apparao, D. and Venkata, Y. (2017), "Integrated model predictive control with reduced switching frequency for modular multilevel converters", *IET Electric Power Applications*, Vol. 11 No. 5, pp. 857 - 863.
- Amin, H., Amir, H.Sh., Navid, N. and David, C.Y. (2015), "Self-tuning indirect adaptive control of non-inverting buck-boost converter", *IET Power Electronics*, Vol. 8 No. 11, pp. 2299 – 2306.
- Alireza, Kh., Mehdi, A. and Mehran, S. (2015), "Reliability evaluation of conventional and interleaved dc-dc boost converters", *IEEE Transactions on Power Electronics*, Vol. 30 No. 10, pp 5821 - 5828.
- H. K.L., T, J.L., L, S.Y. and J.F. Ch. (2012), "Non-inverting buck-boost converter with interleaved technique for fuel-cell system", *IET Power Electronics*, Vol. 5 No. 8, pp. 1379 – 1388
- Mohammad, M., Seyed, H.H., Saeed, Gh., Ebrahim, B., Rasoul, Sh.A. and Tohid, J. (2017), "Six-phase interleaved boost dc/dc converter with high-voltage gain and reduced voltage stress", *IET Power Electronics*, Vol 10 No. 1, pp. 1904 - 1914.
- Z, Z.Y. and M, M.J. (2005), "Implementation and performance evaluation of DSP-based control for constant-frequency discontinues conduction- mode boost PFC front end", *IEEE Transactions on Industrial Electronics*, Vol. 52 No.1, pp. 98 - 107
- Chien, H.T., Yu, Sh.T. and Han, Ch.L. (2015), "A stable mode-transition technique for a digitally controlled non- inverting buck- boost dc- dc converter", *IEEE Transactions on Industrial Electronics*, Vol 62 No. 1, pp.475 - 483.
- Mahmoud, F., Navid, M., Ehsan, A. and Hosein, F. (2017), "High voltage gain interleaved DC-DC converter with minimum current ripple", *IET Power Electronics*, Vol. 10 No. 14, pp. 1924 - 1931.
- Liqin, N., Dean, J.P. and Jerry, L.H. (2012). "High power current sensorless bidirectional 16-phase interleaved dc-dc converter for hybrid vehicle application", *IEEE Transactions on power electronics*, Vol 27 No 3, pp. 1141 - 1151.
- Carlos, R., Javier, C., Angel, C.P. and Abdelali, E.A. (2011), "A non-inverting buck-boost DC-DC switching converter with high efficiency and wide bandwidth", *IEEE Transactions on Power Electronics*, Vol. 26 No. 9, pp. 2490 - 2503.
- Hafiz, F.A., Honnyong, Ch., Ashraf, A.K. and Heung, G.K. (2016), "A novel buck-boost ac-ac converter with both inverting and non-inverting operations and without commutation problem", *IEEE Transactions on Power Electronics*, Vol. 31 No 6, pp. 4241 - 4251.

Corresponding author

Mohsen Karimi "Karimi.fsk@gmail.com"